Bo-Kun Wang, Shao-Yi Wu, Zi-Yi Yuan, Zi-Xuan Liu, Shi-Xin Jiang, Zheng Liu, Zi-Jian Yao, Bao-Hua Teng and Ming-He Wu*

Theoretical Studies of the Spin Hamiltonian Parameters and Local Distortions for Cu^{2+} in Alkaline Earth Lead Zinc Phosphate Glasses

DOI 10.1515/zna-2016-0180
Received May 1, 2016; accepted June 15, 2016; previously published online July 9, 2016

Abstract: The spin Hamiltonian parameters and local structures are theoretically studied for Cu^{2+}-doped alkaline earth lead zinc phosphate (RPPZ, R=Mg, Ca, Sr, and Ba) glasses based on the high-order perturbation calculations for a tetragonally elongated octahedral $3d^9$ cluster. The relative elongation ratios are found to be $\rho \approx 3.2\,\%$, 4.4 %, 4.6 %, and 3.3 % for R=Mg, Ca, Sr, and Ba, respectively, because of the Jahn-Teller effect. The whole decreasing crystal-field strength *Dq* and orbital reduction factor *k* from Mg to Sr are ascribed to the weakening electrostatic coulombic interactions and the increasing probability of productivity of nonbridge oxygen (and hence increasing Cu^{2+}–O^{2-} electron cloud admixtures) under PbO addition, respectively, with increasing alkali earth ionic radius. The anomalies (the largest *Dq* and the next highest *k* among the systems) for R=Ba are attributed to the cross linkage of this large cation in the network. The overall increasing order ($Mg \leq Ba < Ca < Sr$) of ρ is largely due to the decreasing crystal-field strength *Dq* and hence the decreasing force constant of the Cu^{2+}–O^{2-} bonds. The present studies would be helpful to understand local structures and the influences on the optical properties of RPPZ glasses containing copper dopants.

Keywords: Alkaline Earth Lead Zinc Phosphate Glasses; Cu^{2+}; Electron Paramagnetic Resonance.

***Corresponding author: Ming-He Wu,** Department of Applied Physics, School of Physical Electronics, University of Electronic Science and Technology of China, Chengdu 610054, P.R. China, E-mail: wumh68@163.com
Bo-Kun Wang, Zi-Yi Yuan, Zi-Xuan Liu, Shi-Xin Jiang, Zheng Liu and Zi-Jian Yao: School of Yingcai Honors, University of Electronic Science and Technology of China, Chengdu 611731, P.R. China
Shao-Yi Wu and Bao-Hua Teng: Department of Applied Physics, School of Physical Electronics, University of Electronic Science and Technology of China, Chengdu 610054, P.R. China

1 Introduction

Phosphate glasses are both scientifically and technologically important materials because of unique physical properties superior to conventional silicate and borate glasses, e.g. low glass transition and melting temperatures, high thermal expansion coefficients, good biocompatibility, high refractive indices, and low dispersion [1–4]. In addition, phosphate glasses have promising applications in fast ion conductors [5], self-cleaning materials for NH_3 gas absorption [6], important amorphous biomaterials in tissue engineering [7, 8], neural repair of dental and orthopedic cement [9], controlled release of antimicrobials or drugs [10], optical amplifiers, luminescence fibers, and laser hosts [11]. Importantly, the structural versatility using distinct ion exchanges enables phosphate glasses to modify the glass formulation and broadens the range of application fields [12]. For example, the addition of PbO can remarkably improve chemical durability [13] and shielding performance against high-energy radiations [14]. The addition of widely used dopant ZnO yields zinc phosphate glasses and enhances advantageous applications over original phosphate glasses in LED light sources [15], optical waveguides [16], and photoconducting devices [17]. On the other hand, alkaline earth oxide can act as network modifiers in terms of their field strengths [18] and form alkaline earth lead zinc phosphate (RPPZ, R=Mg, Ca, Sr, and Ba) glasses. In particular, transition-metal dopants (e.g. Cu^{2+}) play a crucial role in the physical properties of the glasses. As a typical system among transition-metal ions and convenient dopants in glasses, Cu^{2+} ($3d^9$) has a relatively simpler energy level structure with only one ground state and one excited state in ideal octahedra [19] and usually exhibits Jahn-Teller distortions via the vibration interactions [20, 21]. Thus, divalent copper can be taken as an effective probe to demonstrate the local structural properties of the glass systems due to the typical anisotropic (axial) spectroscopic behaviors arising from the significant orbital angular momentum interactions [19]. In general, local structures of impurity Cu^{2+} (or

other transition-metal ions) in glasses can be investigated using electron paramagnetic resonance (EPR), visible and ultraviolet, infrared, and Raman spectroscopies. Recently, optical and EPR measurements were performed for RPPZ glasses containing copper oxide, and the d-d transition bands and spin Hamiltonian parameters (g factors and hyperfine structure constants) were measured for the impurity Cu^{2+} [22], with anomalies of d-d transition band and $g_{\parallel}$ (i.e. the largest cubic field splitting and the next highest $g_{\parallel}$) for R=Ba. The g factors were calculated from the simple g formulas with various molecular orbital coefficients (α, α', and β) in the previous work [22]. Nevertheless, the above treatments failed to connect with the local structures of impurity Cu^{2+}, and the hyperfine structure constants have not been theoretically analyzed in a consistent way. In fact, the anomalies of EPR and optical spectra for Cu^{2+} in RPPZ (particularly R=Ba) glasses would reveal unique mechanisms dissimilar to the conventional phosphate glasses. Moreover, information of the local structures of the copper dopants may be helpful to understand the properties of these systems. Thus, further theoretical studies for the spin Hamiltonian parameters and local structures of the impurity Cu^{2+} in RPPZ glasses have scientific and practical importance. In this work, the anisotropic g factors and hyperfine structure constants are quantitatively investigated by considering the suitable tetragonal elongation distortions of the octahedral $[CuO_6]^{10-}$ clusters because of the Jahn-Teller effect. The whole tendencies of the d-d transition band, the EPR spectra, and their anomalies for R=Ba are discussed in view of the lead addition and cross linkage.

2 Calculations

Cu^{2+} ions (in the form of CuO dopants) of 0.1 mol% introduced into RPPZ glasses can bring forward the $20RO{\cdot}59.9P_2O_5{\cdot}10Pb_3O_4{\cdot}10ZnO{\cdot}0.1CuO$ (R=Mg, Ca, Sr, Ba) glass systems [22]. Impurity Cu^{2+} ions prefer to occupy suitable octahedral sites in the glass networks and form the $[CuO_6]^{10-}$ clusters. Because Cu^{2+} ($3d^9$) is a Jahn-Teller ion with the ground orbital doublet ^2E_g under ideal octahedral crystal fields, the $[CuO_6]^{10-}$ clusters are subject to the Jahn-Teller effect via the vibrational interactions of the copper-oxygen bonds [7, 23–27]. For example, the two Cu^{2+}–O^{2-} bonds can be elongated along the fourfold axis by a relative elongation ratio ρ, which leads to the tetragonally elongated octahedral $[CuO_6]^{10-}$ clusters (see Fig. 1). As a result, the original twofold orbital degeneracy of cubic ground state ^2E_g is removed, and this level is split into two orbital singlets $^2B_{1g}$ and $^2A_{1g}$, with the former

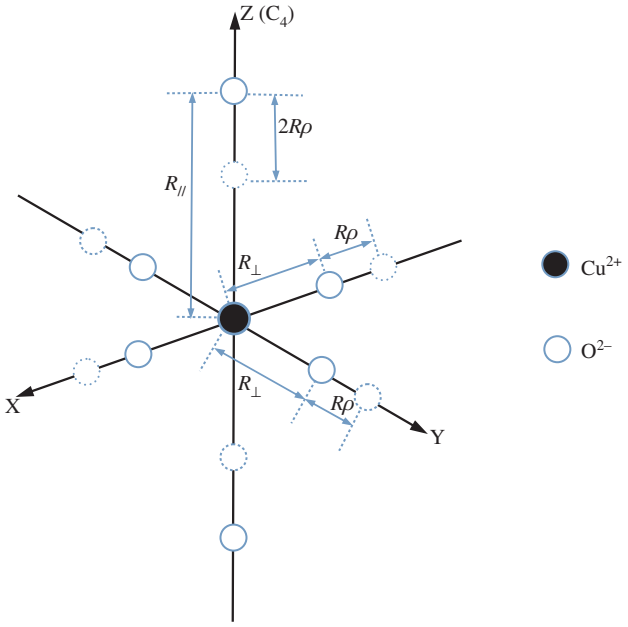

Figure 1: Local structure of the $[CuO_6]^{10-}$ clusters in the RPPZ glasses.

lying lowest and accounting for the measured positive g anisotropies Δg ($=g_{\parallel}-g_{\perp}$) [22, 23]. Then, the original cubic excited orbital triplet $^2T_{2g}$ may be separated into an orbital singlet $^2B_{2g}$ and an orbital doublet ^2E_g.

2.1 Perturbation Formulas of the Spin Hamiltonian Parameters for Tetragonally Elongated Octahedral $3d^9$ Clusters

As mentioned previously, EPR measurements for Cu^{2+} in the RPPZ glasses reveal typical tetragonality of the spin Hamiltonian parameters [22]. To overcome the imperfections of the simple g formulas and various adjustable molecular orbital coefficients in the previous studies [7, 22, 24–26], the high-order perturbation formulas of g factors and hyperfine structure constants for a tetragonally elongated octahedral $3d^9$ cluster are adopted in the present calculations here. Thus, we have the following equations [28–30]:

$$\begin{aligned} g_{\parallel} &= g_s + 8k\zeta/E_1 + k\zeta^2/E_2^{\,2} + 4k\zeta^2/(E_1E_2) \\ &\quad - g_s\zeta^2[1/E_1^{\,2} - 1/(2E_2^{\,2})] + k\zeta^3(4/E_1 - 1/E_2)/E_2^{\,2} \\ &\quad - 2k\zeta^3[2/(E_1^{\,2}E_2) - 1/(E_1E_2^{\,2})] + g_s\zeta^3[1/(E_1E_2^{\,2}) - 1/(2E_2^{\,3})], \\ g_{\perp} &= g_s + 2k\zeta/E_2 - 4k\zeta^2/(E_1E_2) + k\zeta^2(2/E_1 - 1/E_2)/E_2 \\ &\quad + 2g_s\zeta^2/E_1^{\,2}, + k\zeta^3(2/E_1 - 1/E_2)(1/E_2 + 2/E_1)/(2E_2) \\ &\quad - g_s\zeta^3[1/(2E_1^{\,2}E_2) - 1/(2E_1E_2^{\,2}) + 1/(2E_2^{\,3})], \end{aligned}$$

$$A_{\parallel} = P[-\kappa - 4H/7 + (g_{\parallel} - g_s) + 3\Delta g_{\perp}/7],$$
$$A_{\perp} = P[-\kappa + 2H/7 + 11(g_{\perp} - g_s)/14]. \quad (1)$$

Here g_s (≈2.0023) is the spin-only value. k is the orbital reduction factor, reflecting the covalency (or impurity-ligand orbital admixtures) of the systems. ζ and P are the spin-orbit coupling coefficient and the dipolar hyperfine structure parameter of the $3d^9$ ion in the glasses, respectively. κ is the core polarization constant, and H is the reduction factor for the anisotropic hyperfine structure constants because of the axial (tetragonal) distortion [31, 32].

The denominators E_1 and E_2 denote the energy differences between the ground state $^2B_{1g}$ and the excited states $^2B_{2g}$ and ^2E_g, respectively, which can be calculated from the energy matrices for a $3d^9$ ion under tetragonal symmetry [28–30]:

$$E_1 \approx 10Dq,$$
$$E_2 \approx 10Dq - 3Ds + 5Dt. \quad (2)$$

Here Dq is the cubic field parameter, and Ds and Dt are the tetragonal field parameters.

2.2 Tetragonal Field Parameters based on the Superposition Model

Making use of the local geometrical relationship of the tetragonally elongated octahedral $[CuO_6]^{10-}$ clusters, the impurity-ligand bonds parallel and perpendicular to the C_4 axis can be expressed by the reference distance R and the relative elongation ratio ρ (see Fig. 1):

$$R_{\parallel} = R(1 + 2\rho),$$
$$R_{\perp} = R(1 - \rho). \quad (3)$$

Using the superposition model [33–36], the tetragonal field parameters can be determined as follows:

$$Ds = 4\bar{A}_2[(1+2\rho)^{-t2} - (1-\rho)^{-t2}]/7,$$
$$Dt = 16\bar{A}_4[(1+2\rho)^{-t4} - (1-\rho)^{-t4}]/21. \quad (4)$$

Here $t_2 \approx 3$ and $t_4 \approx 5$ are the power law exponents [33]. The relationships $\bar{A}_4 \approx (3/4)\,Dq$ and $\bar{A}_2 \approx 12\bar{A}_4$ [37–40] have been verified suitable in many systems for $3d^n$ ions in octahedral environments, which are also used here. Thus, the local structures in the vicinity of impurity Cu^{2+} are quantitatively correlated to the tetragonal field parameters and hence to the spin Hamiltonian parameters (especially the anisotropy Δg) of the systems.

2.3 Calculations of the Spin Hamiltonian Parameters and Local Structures based on the High-Order Perturbation Formulas

In the calculations of the spin Hamiltonian parameters, the cubic field parameters Dq (≈1224.0, 1210.7, 1189.1, and 1236.1 cm^{-1} [22]) and the orbital reduction factors k (≈0.9115, 0.8967, 0.8864, and 0.9034) are obtained from the optical spectral measurements for Cu^{2+} in the studied systems and similar oxides [22, 41]. The spin-orbit coupling coefficient ζ and the dipolar hyperfine structure parameter P can be calculated from the free-ion values ζ_0 (≈829 cm^{-1} [42]) and P_0 (≈402×10^{-4} cm^{-1} [43]) for Cu^{2+} by multiplying k. From the study of Abragam and Pryce [44], the core polarization constant κ is within the range of 0.26–0.3 for Cu^{2+} in Tutton's salts. In view that the magnitude (or average) of hyperfine structure constants exhibits slightly increasing tendency (Mg < Ca < Sr < Ba [22]), similar increasing κ relevant to the isotropic parts of A factors may be expected. Thus, one can reasonably adopt κ≈0.264, 0.265, 0.271, and 0.272 for R=Mg, Ca, Sr, and Ba, respectively. In the light of the tetragonal elongation distortions for Cu^{2+} in RPPZ glass systems, the reduction factor H can be slightly lower than the ideal value unity for a regular octahedron [31, 32]. From the increasing magnitude (Mg < Ca < Sr < Ba) [22]) of the anisotropy ΔA ($=A_{\parallel} - A_{\perp}$) for hyperfine structure constants, one can suitably take $H \approx 0.895$, 0.912, 0.915, and 0.935 for R=Mg, Ca, Sr, and Ba, respectively. Thus, there is only one unknown quantity (i.e. the relative elongation ratio ρ) in the formulas of the spin Hamiltonian parameters. Inserting the relevant values into (1) and matching the calculated anisotropies Δg to the experimental data, the optimal relative elongation ratios,

$$\rho \approx 3.2\ \%,\ 4.4\ \%,\ 4.6\ \%,\ \text{and}\ 3.3\ \%, \quad (5)$$

are obtained for R=Mg, Ca, Sr, and Ba, respectively. The corresponding spin Hamiltonian parameters (Calc.[c]) are listed in Table 1.

2.4 Analysis of *g* Factors based on the Previous Simple *g* Formulas with Various Molecular Orbital Coefficients

As mentioned before, the treatments of g factors were performed based on the simple g formulas with various molecular orbital coefficients (α, α', and β) in the previous work [22], with the corresponding theoretical g factors (Calc.[a]) shown in Table 1. To further examine the covalency of the studied $[CuO_6]^{10-}$ clusters in the RPPZ glasses, theoretical analysis is used here on the basis of the more

Table 1: The g factors and hyperfine structure constants (in 10^{-4} cm^{-1}) for Cu^{2+} in the RPPZ glasses.

R	$g_{\parallel}$	$g_{\perp}$	$A_{\parallel}$	$A_{\perp}$
Mg				
Calc.[a]	2.389	2.112	–	–
Calc.[b]	2.392	2.092	–	–
Calc.[c]	2.464	2.100	−100.4	25.2
Expt. [22]	2.464	2.095	−100.5	25.2
Ca				
Calc.[a]	2.366	2.105	–	–
Calc.[b]	2.355	2.092	–	–
Calc.[c]	2.449	2.093	−108.1	24.0
Expt. [22]	2.449	2.093	−108.2	24.0
Sr				
Calc.[a]	2.355	2.104	–	–
Calc.[b]	2.338	2.092	–	–
Calc.[c]	2.447	2.092	−110.8	21.5
Expt. [22]	2.447	2.092	−110.0	22.0
Ba				
Calc.[a]	2.371	2.111	–	–
Calc.[b]	2.368	2.093	–	–
Calc.[c]	2.448	2.097	−116.3	25.2
Expt. [22]	2.448	2.097	−116.0	25.0

[a]Calculations of g factors based on the simple g formulas and the molecular orbital coefficients α, α', and β of Ref. [22].

[b]Calculations of g factors based on the simple g formulas and the molecular orbital coefficients α, β, and β_1 of Ramadevudu et al. [45].

[c]Calculations of the spin Hamiltonian parameters in present work based on the high-order perturbation formulas in (1) and the optimal tetragonal elongation ratios ρ in (5).

conventional molecular orbital coefficients (α, β, and β_1) of Ramadevudu et al. [45]. Here α indicates the in-plane σ-bonding with the $d_{x^2-y^2}$ orbitals, β describes the out-of-plane π-bonding with the d_{xz} and d_{yz} orbitals, and β_1 demonstrates the in-plane π-bonding with the d_{xy} orbitals, respectively; Γ_σ and Γ_π reflect the normalized covalency coefficients of Cu^{2+}–O^{2-} bonds in σ and π planes, respectively [45]. The detailed expressions of these quantities can be expanded in terms of the measured spin Hamiltonian parameters ($g_{\parallel}$, $g_{\perp}$, and $A_{\parallel}$) as follows [45]:

$$\alpha^2=-\frac{A_{\parallel}}{P_0}+(g_{\parallel}-g_{\perp})+\frac{3}{7}(g_{\perp}-g_s)+0.04,$$
$$\beta^2=\frac{(g_{\perp}/g_s-1)(\Delta E_{xz,yz})}{\zeta_0\alpha^2},$$
$$\beta_1^2=\frac{(g_{\parallel}/g_s-1)(\Delta E_{xy})}{4\zeta_0\alpha^2},$$
$$\Gamma_\pi=200(1-\beta_1^2)(\%),$$
$$\Gamma_\sigma=200\frac{(1-S)(1-\alpha^2)}{1-2S}(\%), \quad (6)$$

where $\Delta E_{xz,yz}$ can be calculated as follows [45]:

$$\Delta E_{xz,yz}=2K^2\zeta_0/(g_{\perp}-g_s). \quad (7)$$

Here S (≈0.076 [45]) is the overlap integral between the copper 3d orbitals and the normalized ligand orbitals, and K (≈0.77 [45]) denotes the covalency factor. For consistency, the free-ion values ζ_0 (≈829 cm^{-1} [42]) and P_0 (≈402×10^{-4} cm^{-1} [43]) for the calculations of the spin Hamiltonian parameters in Section 2.3, which are slightly different from those (≈828 cm^{-1} and 360×10^{-4} cm^{-1}) of the previous works [22, 45], are applied in the analysis of g factors based on the simple g formulas and the molecular orbital coefficients here. Inputting the related experimental data of $g_{\parallel}$, $g_{\perp}$, $A_{\parallel}$ and E_1 (=ΔE_{xy}) [22], the molecular orbital coefficients and the normalized covalency coefficients as well as the averages $\chi=(\alpha+\beta+\beta_1)/3$ and $\Gamma=(\Gamma_\sigma+\Gamma_\pi)/2$ are obtained and shown in Table 2. The corresponding theoretical g factors (Calc.[b]) are also collected in Table 1 for comparison.

3 Discussion

From Table 1, one can find that the theoretical spin Hamiltonian parameters (Calc.[c]) for Cu^{2+} in the RPPZ glasses based on the high-order perturbation formulas in (1) and the relative elongation ratios in (5) show good agreement with the measured results. However, the calculated g factors (Calc.[a] or Calc.[b]) based on the simple g formulas and the adjusted molecular orbital coefficients (α, α', and β or α, β, and β_1) based on the formulas of Sreehari Sastry and Rupa Venkateswara Rao [22] or Ramadevudu et al. [45] are not so well. Moreover, the local distortions around impurity Cu^{2+} in the glass systems are also quantitatively obtained. There are several points that may be discussed here.

(1) Except the anomalous increases for R=Ba, both the cubic field parameter Dq [23] and the orbital reduction factor k exhibit overall decreasing tendencies

Table 2: The molecular orbital coefficients α, β, and β_1, the normalized covalency coefficients Γ_π and Γ_σ, and the averages χ (=$(\alpha+\beta+\beta_1)/3$) and Γ (=$(\Gamma_\pi+\Gamma_\sigma)/2$) based on the formulas of Ramadevudu et al. [45] for Cu^{2+} in the RPPZ glasses.

R	α	β	β_1	χ	Γ_π (%)	Γ_σ (%)	Γ (%)
Mg	0.892	0.824	0.956	0.890	21	44	33
Ca	0.893	0.822	0.913	0.876	37	43	40
Sr	0.895	0.820	0.890	0.868	44	44	44
Ba	0.905	0.817	0.918	0.880	35	39	37

(Mg > Ca > Sr) with increasing alkaline earth ionic radius, consistent with those (Li > Na > K) for the same $[CuO_6]^{10-}$ clusters in similar alkali lead tetraborate glasses $90R_2B_4O_7 \cdot 9PbO \cdot CuO$ (R=Li, Na, K) [23, 24]. Physically, the overall decreasing *Dq* may be ascribed to the weakening electrostatic coulombic interactions with increasing alkali or alkaline earth ion radius [24, 25]. The lower *Dq* values for RPPZ glasses than those (≈1275.1–1302.0 cm^{-1}) for alkali lead tetraborate glasses [25] are attributable to the lower stability of the network and hence weaker Cu^{2+}–O^{2-} bonding in the former. On the other hand, the overall decreasing tendency (Mg > Ca > Sr) of *k* may be illustrated by the increasing probability of productivity of nonbridge oxygen (NBO) and hence the enhancing Cu^{2+}–O^{2-} electron cloud admixtures with increasing alkali earth ionic radius under PbO addition in the network [7, 26]. Interestingly, the previously mentioned decreasing rule of *k* from Mg to Sr is in accordance with the whole decreasing rule of χ $(=(\alpha+\beta+\beta_1)/3)$ of the molecular orbital coefficients and the increasing rule of the average Γ $(=(\Gamma_\pi+\Gamma_\sigma)/2)$ of the normalized covalency coefficients based on (6) and (7) of Ramadevudu et al. [45] (see Tab. 2). Further, both the orders of χ (Mg > Ba > Ca > Sr) and Γ (Mg < Ba < Ca < Sr) actually reveal the order of covalency (Mg < Ba < Ca < Sr) or *k* (Mg > Ba > Ca > Sr) of the systems. On the other hand, the rough relationship $\Gamma_\pi \leq \Gamma_\sigma$ for Cu^{2+} in the RPPZ glasses is supported by the previous studies of Sreehari Sastry and Rupa Venkateswara Rao [22] and can be regarded as suitable. Thus, the systems may be treated as dominantly ionic, with the percentage of the covalency of approximately 9 %–13 %. In addition, the orbital reduction factors *k* for the present systems are higher than those (≈0.774, 0.762, and 0.756) for the similar $90R_2B_4O_7 \cdot 9PbO \cdot CuO$ glasses [23], possibly because of the weaker covalency of in-plane π bonding in phosphate glasses than borate glasses [46].

(2) Despite the previously mentioned overall decreasing tendencies of *Dq* and *k* from Mg to Sr, the anomalies are found for R=Ba, i.e. both quantities show the abrupt increases related to SrPPZ, yielding the largest *Dq* (Ba > Mg > Ca > Sr) and the next highest *k* (Mg > Ba > Ca > Sr) among the systems. The anomalies can be attributed to the cross linkage of Ba^{2+} in the network because of its large ionic radius [22]. Ba^{2+} at 20 mol% may tend to coordinate with more oxygen ions and form dominantly ionic bonding owing to the high ionicity. Thus, the electron cloud admixture (or covalency) can considerably decrease and induce the increases of ionicity and effective charge Q_{eff} of the oxygen ions bonding to both Ba^{2+} and impurity Cu^{2+}. As a result, the covalency of $[CuO_6]^{10-}$ clusters in BaPPZ exhibits a significant decrease and yields the next highest *k* among the systems, consistent with the next largest χ and the next smallest Γ (see Tab. 2). As for the cubic field parameter, the relationship $Dq \propto Q_{eff}$ *k* based on the point charge model is approximately held for an octahedral cluster [19]. For R=Mg, Ca, and Sr, the effective charge Q_{eff} of ligand oxygen may largely remain unchanged, and thus the decreasing *k* brings forward the decreasing order (Mg > Ca > Sr) of Dq for the three systems. As regards BaPPZ, however, the increases of both *k* and Q_{eff} arising from the cross linkage can yield a remarkable increase of Dq and lead to the resultant order Ba > Mg > Ca > Sr of *Dq*. Finally, the overall increasing order (Mg ≤ Ba < Ca < Sr) of the relative tetragonal elongation ratio ρ suitably reflects the increasing Jahn-Teller tetragonal elongations via the vibration interactions because of the decreasing crystal-field strength *Dq* (or force constant of the Cu^{2+}–O^{2-} bonds).

(3) In light of (1), the high *k* (≈0.9–1) and hence the large ζ as well as the moderate *Dq* (i.e. the denominator E_1) may account for the relatively large magnitudes (averages) of *g* factors. The moderate local relative elongation ratios ρ (≈3 %–5 %) for Cu^{2+} in RPPZ glasses can be illustrated by the measured EPR spectra characterized by the moderate positive anisotropies Δg (≈0.34 [22]). In addition, the moderate ρ due to the Jahn-Teller effect can induce moderate negative *Ds* and *Dt* and hence the moderate denominator E_2, leading to the relatively larger $g_\perp$ (≈2.09 [22]) for the present RPPZ glasses than those ($g_\perp \approx 2.04$ [23]) with much larger relative elongation ratios (≈18 %–30 % [23]) for the alkali lead tetraborate glasses. Similar moderate relative tetragonal elongations (≈6.8 % and 8.9 % [47]) are found for Cu^{2+} in $LiRbB_4O_7$ and $NaRbB_4O_7$ glasses. On the other hand, normally merely absolute values were experimentally determined for hyperfine structure constants in EPR measurements [22]. The present calculations and various observed hyperfine structure constants [43] for Cu^{2+} in oxides reveal that the signs of $A_\parallel$ and $A_\perp$ are negative and positive, respectively. This may be ascribed to the larger negative isotropic terms related to κ than the positive anisotropic ones related to the *g*-shifts and *H* [see (1)]. Further, the increasing orders (Mg < Ca < Sr < Ba) of κ and *H* are suitably responsible for those of the average $(=|A_\parallel + 2A_\perp|/3)$ and anisotropy $(=|A_\parallel| - |A_\perp|)$ of the hyperfine structure constants and can be regarded as reasonable in physics.

4 Summary

The spin Hamiltonian parameters and local structures are theoretically investigated for Cu^{2+} in RPPZ glasses. The relative tetragonal elongation ratios ρ are found to be approximately 3.2 %, 4.4 %, 4.6 %, and 3.3 % for R=Mg, Ca, Sr, and Ba, respectively, because of the Jahn-Teller effect. The whole decreasing crystal-field strength Dq and orbital reduction factor k from Mg to Sr can be ascribed to the weakening electrostatic coulombic interactions and the increasing probability of productivity of NBO (the enhancing Cu^{2+}–O^{2-} electron cloud admixtures), respectively, under PbO addition with increasing alkali earth ionic radius. The anomalies (i.e. the largest Dq and the next highest k among all the systems) for R=Ba with the abrupt increases related to R=Sr are attributed to the cross linkage of Ba^{2+} in the network because of its large ionic radius. The overall increasing order ($Mg \leq Ba < Ca < Sr$) of ρ is illustrated by the decreasing crystal-field strength Dq (force constant of the Cu^{2+}–O^{2-} bonds). The present studies would be helpful to understand local structures and the relationships with properties of RPPZ glasses containing copper dopants.

Acknowledgments: This work was financially supported by "the Sichuan Province Academic and Technical Leaders Support Fund" (grant no. Y02028023601032) and "the Fundamental Research Funds for the Central Universities" (grant no. ZYGX2014J136).

References

[1] B. Eraiah and S. G. Bhat, J. Phys. Chem. Solids **68**, 581 (2007).
[2] A. Marino, S. Arrasmith, L. Gregg, S. Jacobs, G. Chen, et al., J. Non-Cryst. Solids **289**, 37 (2001).
[3] S. F. Ismail, M. R. Sahar, and S. K. Ghoshal, Mater. Charact. **111**, 177 (2016).
[4] M. R. Dousti and R. J. Amjad, J. Non-Cryst. Solids **420**, 21 (2015).
[5] X. Xu, Z. Wen, X. Yang, J. Zhang, and Z. Gu, Solid State Ionics **177**, 2611 (2006).
[6] Y. Daiko, H. Yajima, T. Kasuga, Y. Daiko, H. Yajima, et al., J. Eur. Ceram. Soc. **28**, 267 (2008).
[7] S. Cetinkaya Colak and E. Aral, J. Alloys Compd. **509**, 4935 (2011).
[8] S. V. Dorozhkin, Acta Biomater. **6**, 4457 (2010).
[9] M. Uo, M. Mizuno, and Y. Kuboki, Biomaterials **19**, 2277 (1999).
[10] A. A. Chavez-Pirson, In: Workshop on Specialty Optical Fibers and Their Applications (WSOF-10), International Society for Optics and Photonics, 2010 78390K-1-4.
[11] D. M. Pickup, R. J. Newport, and J. C. Knowles, J. Biomater. Appl. **26**, 613 (2012).
[12] S. Lanfredi, P. S. Saia, R. Lebullenger, and A. C. Hermandes, Solid State Ionics **146**, 329 (2002).
[13] Y. M. Moustafa and A. El-Adawy, Phys. Status Solidi **179a**, 83 (2000).
[14] B. C. Sales and L. A. Boatner, Mater. Lett. **2**, 301 (1984).
[15] R. Martínez-Martínez, A. Speghini, M. Bettinelli, C. Falcony, and U. Caldiño, J. Lumin. **129**, 1276 (2009).
[16] B. F. Luke, J. W. Jon, T. Neil, T. R. Signo, K. B. Richard, et al., J. Appl. Phys. **112**, 023109 (2012).
[17] Z. A. Talib, W. M. Daud, and E. Z. M. Tarmizi, J. Phys. Chem. Solids **69**, 1969 (2008).
[18] M. M. Smedskjaer, R. E. Youngman, and J. C. Mauro, J. Non-Cryst. Solids **381**, 58 (2013).
[19] C. P. Poole, Electron Spin Resonance: A Comprehensive Treatise on Experimental Techniques, 2nd ed., Interscience Publishers, New York 1996.
[20] S. O. Graham and R. L. White, Phys. Rev. **10b**, 4505 (1974).
[21] Y. V. Yablokov and T. A. Ivanova, Coord. Chem. Rev. **190–192**, 1255 (1999).
[22] S. Sreehari Sastry and B. Rupa Venkateswara Rao, Physica **434b**, 159 (2014).
[23] M. Q. Kuang, S. Y. Wu, G. L. Li, and X. F. Hu, Mol. Phys. **113**, 698 (2014).
[24] J. L. Rao, G. Sivaramaiah, and N. O. Gopal, Physica **349b**, 206 (2014).
[25] R. K. Brow and D. R. Tallent, J. Non-Cryst. Solids **222**, 396 (1997).
[26] J. L. Pascual, L. Seijo, and Z. Barandiran, J. Chem. Phys. **103**, 4841 (1995).
[27] R. W. Reynolds, L. A. Boatner, M. M. Abraham, and Y. Chen, Phys. Rev. **10b**, 3802 (1974).
[28] S. Y. Wu, H. M. Zhang, P. Xu, and S. X. Zhang, Spectrochim. Acta **75a**, 230 (2010).
[29] M. Q. Kuang, S. Y. Wu, X. F. Hu, and B. T. Song, Z. Naturforsch. **68a**, 442 (2013).
[30] S. Y. Wu, J. S. Yao, H. M. Zhang, and G. D. Lu, Int. J. Mod. Phys. **21b**, 3250 (2007).
[31] M. T. Barriuso, J. A. Aramburu, and M. Moreno, J. Phys. Condens. Matter **14**, 6521 (2002).
[32] Y. Q. Xu, S. Y. Wu, M. Q. Kuang, X. F. Hu, and C. C. Ding, J. Non-Cryst. Solids **432**, 535 (2016).
[33] D. J. Newman and B. Ng, Rep. Prog. Phys. **52**, 699 (1989).
[34] S. Y. Wu, X. Y. Gao, and H. N. Dong, Mater. Lett. **60**, 1319 (2006).
[35] J. Z. Lin, S. Y. Wu, Q. Fu, and H. M. Zhang, Mod. Phys. Lett. **21b**, 737 (2007).
[36] S. Y. Wu and H. N. Dong, J. Lumin. **119–120**, 517 (2006).
[37] Y. X. Hu, S. Y. Wu, and X. F. Wang, Philosoph. Mag. **90**, 1391 (2010).
[38] H. M. Zhang, S. Y. Wu, M. Q. Kuang, and Z. H. Zhang, J. Phys. Chem. Solids **73**, 846 (2012).
[39] J. Z. Lin, S. Y. Wu, Q. Fu, and G. D. Lu, Z. Naturforsch. **61a**, 583 (2006).
[40] H. N. Dong and X. S. Liu, Mol. Phys. **113**, 492 (2015).
[41] A. S. Chakravarty, Introduction to the Magnetic Properties of Solids, Wiley-Interscience Publication, New York 1980.

[42] J. S. Griffith, The Theory of Transition-Metal Ions, Cambridge University Press, London 1964.
[43] B. R. McGarvey, J. Phys. Chem. **71**, 51 (1967).
[44] A. Abragam and M. H. I. Pryce, Proc. Roy. Soc. (London) **206a**, 164 (1951).
[45] G. Ramadevudu, M. Shareefuddin, N. S. Bai, M. L. Rao, and M. N. Chary, J. Non-Cryst. Solids **278**, 205 (2000).
[46] H. Hosono, H. Kawazoe, and T. Kanazawa, J. Non-Cryst. Solids **33**, 103 (1979).
[47] H. M. Zhang and X. Wan, J. Non-Cryst. Solids **361**, 43 (2013).